

Very Early Photometry of SN 1998S: Physical Parameters and Date of Explosion

Poon, H.¹, Pun, J. C. S.¹, Lam, T. Y.², Qiu, Y. L.³, and Wei, J. Y.³

¹ Department of Physics, University of Hong Kong, Pokfulam Road, Hong Kong, PR China
e-mail: china_108@yahoo.com

² Institute for the Physics and Mathematics of the Universe, University of Tokyo, Kashiwa, Chiba 277-8583, Japan

³ National Astronomical Observatories, Chinese Academy of Science, 20a Datun road, Chaoyang District, Beijing, PR China

Preprint online version: August 23, 2018

ABSTRACT

Context. We present very early optical lightcurves beginning 10 days before maximum of the Type IIn supernova 1998S, covering the first four months after discovery.

Aims. We examine the light evolution and try to compare the lightcurves to two analytical models (Nakar & Sari(2010) and Rabinak & Waxman(2011)) for a red supergiant star.

Methods. The photometry was carried at the 60-cm telescope of the Xinglong Station of China. Broadband filters Johnson's *B*, *V* and Cousins' *R* were used.

Results. The magnitude rose for the first few days and then dropped slowly afterwards. The two different models we use can fit the early lightcurves very well. The explosion date derived from the models is within the range of 1998 March 1.34 - 2.64 (JD 2450873.84 - JD 2450875.14.) The radius of the progenitor is found to be $\sim 300 R_{\odot}$ and $\sim 2000 R_{\odot}$ for the model of Nakar & Sari(2010) and Rabinak & Waxman(2011) respectively. The constraint on mass and energy is not strong. The ranges of these two parameters are within that of a red supergiant.

Key words. supernovae: general – supernovae: individual (SN 1998S)

1. Introduction

SN 1998S was discovered by BAO on March 2.68, 1998 (Li & Li 1998). This supernova lies in NGC 3877. There was no sign of supernova on the CCD image taken on Feb 23.7 (Leonard et al. 2000). It is one of the brightest Type IIn supernova observed so far.

Type II supernovae are characterized by the presence of hydrogen in the spectrum. According to the shape of light curves, they can be further classified as II-P and II-L (Barbon et al. 1979). The former show a plateau while the latter show a linear decay. Schlegel(1990) defined a new subclass of Type IIn. Their spectra show narrow emission lines with weak or no P - Cygni absorption component.

Early-time lightcurves are especially important in which they can be used to test different models to constrain the progenitor's parameters. Modjaz et al. (2009) compared their early-time bolometric lightcurves of 2008D to the model of Waxman et al. (2007) and also that of Chevalier & Fransson (2008). They estimated the radius to be $1.2 \pm 0.7 R_{\odot}$ for the former model and $12 \pm 7 R_{\odot}$ for the later one. Gezari et al. (2010) applied the model of Nakar and Sari(2010, hereafter NS10) and RW11(2011, hereafter RW11) to the early(< 3 d) UV/optical lightcurves of SN IIP 2010aq. NS10 can fit the lightcurves well with an offset of -1.5 mag. Combining all the constraints, they found the radius of the progenitor to be $700 \pm 200 R_{\odot}$. For RW11, they fit the lightcurves with parameters within the constraints. The fit agrees with the data well at the time of the first detection of the source, but the temperature evolution is slower.

Filippenko & Moran (1998) first presented the spectra of SN 1998S and found it to be a type II supernova. Due to the presence of narrow H α emission lines (Filippenko & Moran 1998), they suggested that the supernova belongs to the type IIn. From the *BV* light curves and spectroscopic behavior, Liu et al. (2000) indicated a similarity between the supernova and Type IIL SN 1979C. Leonard et al. (2000) found a high degree of linear polarization in their spectropolarimetric observations which implied asphericity for the continuum-scattering medium. Chandra observations (Pooley et al. 2002) of the supernova at the age of three show overabundant heavy elements. Pozzo et al. (2004) presented late-time near-infrared and optical spectra of the supernova. From the shape and evolution of the H α and He I line profiles, they noticed a powerful interaction with a RSG wind. The variable component found in optical/UV spectra indicates slow-moving circumstellar outflows originating from the red supergiant progenitor (Bowen et al. 2000).

Fassia et al. (2000) presented contemporaneous photometry in the optical and infrared bands between day 11 to 146 after discovery and reported a high IR excess at day 130. The result was interpreted as due to thermal emission from dust grains in the vicinity of the supernova. Liu et al. (2002) observed the supernova in the *BVR* bands and found the light curves typical of a SN II-L.

In this paper, we present optical photometry of SN 1998S spanning the first four months. We reanalyze the data from Liu et al. (2000) using the same data reduction method. We extend the early light curves of SN 1998S by adding a new data point taken on the day of discovery. We compare the new lightcurves

to two models proposed by NS10 and RW11. These two models are for early supernovae lightcurves. We have enough data to use model fits to constrain the parameters and the date of explosion of the supernova.

2. Observations and Results

Our photometric observations were carried out at the 60 cm telescope located at the Xinglong Station of the National Astronomical Observatories of China (NAOC). The TI 215 CCD camera has 1024×1024 square pixels, a field of view of $16.8' \times 16.8'$, a gain of $11.6 \text{ e}^-/\text{ADU}$ and readout noise of 8 e^- . The exposure time was about 120 s when the SN was around maximum and 300 s when it was dim. For the first 10 days after discovery, there are 6 data points taken, with the first data point taken on the day of discovery (1998 March 2). Altogether, data of 32 nights were obtained, spanning four months. Standard *BVR* filters were used except for the discovery data point, which was unfiltered.

After flat-fielding, bias, and dark corrections, aperture photometry was performed using the *apphot* task of IRAF. The comparison star we use is GSC 3452-1061. Its magnitudes are $B = 13.06 \pm 0.03$, $V = 12.57 \pm 0.007$ and $R = 12.28 \pm 0.008$ (Fassia et al. 2000). For the unfiltered data point, we use the following CCD transformation formula provided by BAO (private communication):

$$i = I + i_1 + i_2 X_i + i_3 (V - I) + i_4 X_i (V - I) \quad (1)$$

where i is the instrumental unfiltered magnitude, I is the standard unfiltered magnitude and V is the standard V band photometry. As differential photometry would be applied, the values of the coefficients i_1 and i_2 are neglected and $i_3 = -0.039 \pm 0.021$ and $i_4 = 0$. Then equation (1) becomes

$$i_{SN} - i_{star} = I_{SN} - I_{star} + i_3 (V_{SN} - I_{SN}) - i_3 (V_{Star} - I_{Star}) \quad (2)$$

We take the unfiltered magnitude as the standard R magnitude by approximation. Since the value of i_3 is small and the comparison star has similar V and R magnitudes, the last term $i_3 (V_{Star} - I_{Star}) \approx 0.01$ and is neglected. To estimate the value of this term, $i_3 (V_{SN} - I_{SN})$, we first calculate the temperatures of the supernova by converting our *BVR* data to fluxes and then perform a blackbody fit. The results and the errors are listed in the last column of table 1. We then extrapolate the temperature by performing an exponential fit and find the temperature to be $27300 + 12200/(t - 10500) \text{ K}$ for the unfiltered data point. The results are shown in fig. 1. By assuming a blackbody spectrum, at $T = 27300 + 12200/(t - 10500) \text{ K}$, the magnitude difference between V and R bands is $\sim 0.18 - 0.27$. Thus, the term $i_3 (V_{SN} - I_{SN})$ is ~ 0.01 at maximum and can be neglected. We also try to determine this temperature by performing a 3rd order polynomial. A result of $25000 \pm 8900 \text{ K}$ is found. Altogether, the error in neglecting the last two terms of equation (2) should not be more than 0.02, plus the error of the instrumental magnitude given by IRAF, which is 0.09, the final error of the unfiltered data point is ~ 0.11 . The photometry for all bands is listed in Table 1. The numbers in the brackets represent the errors. Figure 2 shows the lightcurves in the *BVR* bands. Constants are added to individual light curve. The photometry data from Fassia et al. (2000) are included for comparison.

3. Comparison with Analytical Models

There are different models which can explain the lightcurves of supernovae. In the 80s, Arnett (1980, 1982) developed an ana-

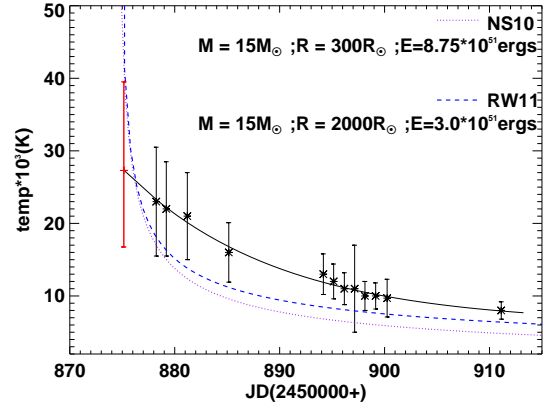


Fig. 1. Exponential fit (black solid line) of the temperatures of 1998S. The red dot represents the extrapolated temperature of the discovery data point. The purple dotted line represents the analytical model of NS10 and the blue dashed line represents that of RW11. The best fitting parameters of these two models are used.

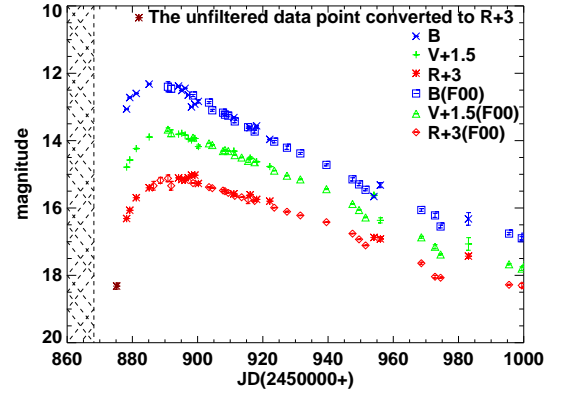


Fig. 2. *BVR* light curves of SN 1998S. Data from Fassia et al. (2000) (F00) are included for comparison. The dashed straight line on JD = 2450868.2 indicates the earliest possible date of explosion.

lytical model of radioactive decay diffusion. In this model, the radioactive decay of nickel and cobalt is the main power source which diffuses out from the expanding envelope. This model can successfully model the late ($t = 20 - 1500$ days) bolometric lightcurves of 1987A (Arnett & Fu 1989). Later in the 90s, Chugai (1992) suggested a shock-wind interactions model for type II supernovae at a late stage. The shock interaction of the supernova shell with the wind of the presupernova is the main source of energy for this model. The anomalous late-time lightcurves of SN 1987F and SN 1988Z can be duplicated in the model. More recently, Chevalier & Fransson (2008) proposed a simple model for the optical/ultraviolet emission from shock breakout. Since this model requires a small radius progenitor, it is applicable to Type Ib/c supernovae.

We compare our lightcurves to two analytical models for an RSG for early supernova lightcurves and try to constrain the progenitor's parameters. NS10 takes into account photon-gas coupling and deviations from thermal equilibrium. The breakout is observed and then rises to a maximum luminosity in a very short time (< 1 day). Immediately after the breakout, the luminosity keeps rising until a diffusion time t_0 (this is the luminosity of a radiation that leaks from the center of a static slab). Then after t_0 , light travel time effects are included and the luminosity keeps

on rising and reaches a maximum value at R_{star}/c . At R_{star}/c , the lightcurve starts to decay in the planar stage(i.e., before the expanding gas doubles its radius) and then it rises again at the transition between the planar and spherical phase. The luminosity then drops until the frequency range reaches its maximum in the blackbody spectrum. The effects of recombination are not included, which is considered to be important only at a later stage. RW11 focuses on the UV/O emission around ~ 1 day following the X-ray outburst. The breakout phase is not considered. This model extends the analytic model of Waxman et al. (2007) to include an approximate description of the time dependence of the opacity(due mainly to recombination), and of the deviation of the emitted spectrum from a black body spectrum. RW11 applied their model to the early UV/O lightcurves of the type Ib SN2008D and of the type IIP SNLS-04D2dc and found the results consistent with the predictions of this model.

3.1. Date of Explosion

We first try to determine the date of explosion using both models. Figure 3 shows the results of the best fits with different explosion dates. We only consider fitting our lightcurves up to day 10 since both models are for early lightcurves and do not take into account the production of nickel as a source of power supply at a later stage. From the figure, the explosion date JD 2450874.34(1998 March 1.84) gives the best fit for NS10. The results of the fit with $t_{exp} = \text{JD } 2450873.84$ and JD 2450874.84 are still satisfactory, only with considerable deviation from the first data point. For RW11, $t_{exp} = \text{JD } 2450874.64$ (1998 March 2.14) gives the best fit. $t_{exp} = \text{JD } 2450874.14$ shows some deviation and $t_{exp} = \text{JD } 2450875.14$ cannot fit the data at all. Hence, we conclude that the explosion date is within the range of JD 2450873.84 - JD 2450875.14(1998 March 1.34 - 2.64). The first data point was taken on day 0.69(taking the explosion date to be JD 2450874.49, the average of the best results derived from both models) after explosion. From the consistency between model predictions and the evolution of photospheric radius, Chugai (2001) assumed the date of explosion to be 1998 February 24.7 UT. He calculated the bolometric luminosity, radius and velocity of the thin shell of the supernova using a combined model which includes a model with ejecta-wind interaction(Chugai 1992) and one without wind(Arnett 1980;1982). For the early data(before \sim day 20) of the bolometric luminosity(Fassia et al. 2000, the authors derived the bolometric luminosity by performing a blackbody fit to their *UBVRIJHK* data), the analytical lightcurves even make a better fit under the new date of explosion. Originally, the radius of the thin shell derived from this model can fit the empirical radii well(Fassia et al. 2000) but this result is a little worse if the date of explosion is shifted backward by ~ 5 days. As for the velocity of the thin shell, this is not affected at all since the model predicts a steady value.

3.2. Parameters of the Progenitor

Figure 4 shows the results of the best fit for NS10 and RW11 for an RSG with different radii and the best corresponding combinations of mass and energy. The residuals are listed in Table 2. The first four data points were taken in the very early phase and can very well constrain the parameters. All fits are satisfactory up to day ~ 6 for both models. For NS10, $R = 300R_{\odot}$, $M = 15M_{\odot}$ and $E = 8.75 \times 10^{51}$ ergs can fit the data up to day ~ 25 . For smaller radius, the luminosity first drops to a lower one and then rises less sharply compared with a larger radius. For RW11,

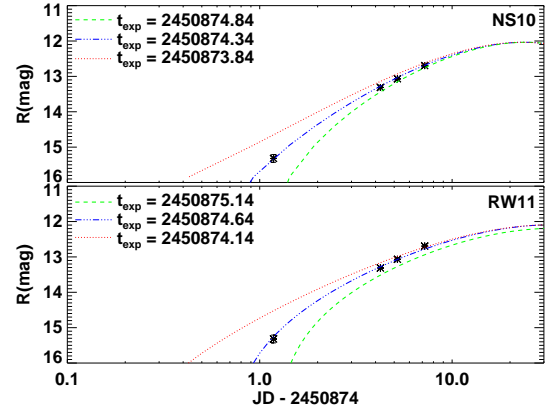


Fig. 3. The best fit of NS10(top panel with $E = 8.75 \times 10^{51}$ ergs, $M = 15M_{\odot}$, $R = 300R_{\odot}$) and RW11(bottom panel with $E = 3.0 \times 10^{51}$ ergs, $M = 15M_{\odot}$, $R = 2000R_{\odot}$) for different explosion dates.

$R = 2000R_{\odot}$, $M = 15M_{\odot}$ and $E = 3.0 \times 10^{51}$ ergs fit all the data best. The luminosity of the lightcurves of this model all show similar tendency in the very early phase but then it rises more sharply for larger radii at a later stage.

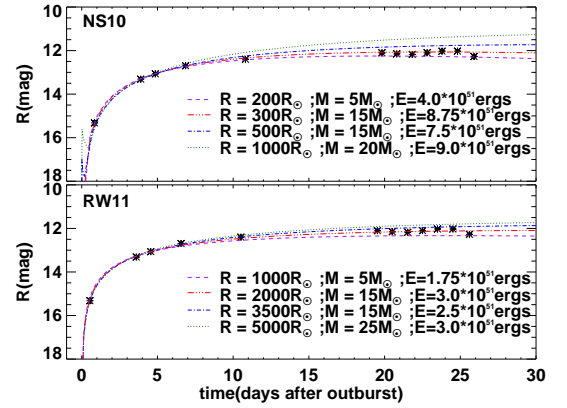


Fig. 4. Zoom in of the optical lightcurves of SN 1998S in comparison to the analytical model of NS10(top panel) and RW11(bottom panel) with different radii and the best corresponding combinations of mass and energy. The dates of explosion for NS10 and RW11 in the figure are JD 2450874.34 and JD 2450874.64 respectively.

We try to investigate the importance of radius in both models by using different radii and fixed mass and energy to fit the data. In figure 5, we show the lightcurves for NS10 and RW11 with fixed mass and energy and different radii. The lightcurves begin to differ in the very early phase for both models, especially for RW11, which begin to differ within one day after explosion. The magnitude for a smaller radius begins to drop sooner than that for a larger radius in both models.

In figure 6, we show the lightcurves for NS10 and RW11 with fixed radius and energy and varying mass. A smaller mass results in brighter magnitudes for both models. The different lightcurves show similar tendency. They mainly differ in magnitudes. By adding a constant, all lightcurves can fit the data.

We plot the lightcurves for both models with fixed mass and radius and different energies in figure 7. In RW11, a small change in energy results in larger differences in magnitudes than

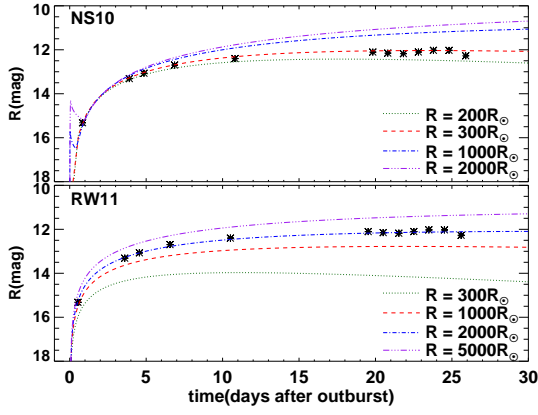


Fig. 5. Zoom in of the optical lightcurves of SN 1998S in comparison to the analytical model of NS10(top panel with $M = 15M_{\odot}$ and $E = 8.75 \times 10^{51}$ ergs) and RW11(bottom panel with $M = 15M_{\odot}$ and $E = 3.0 \times 10^{51}$) with different radii. The dates of explosion for NS10's and RW11's models in the figure are JD 2450874.34 and JD 2450874.64 respectively.

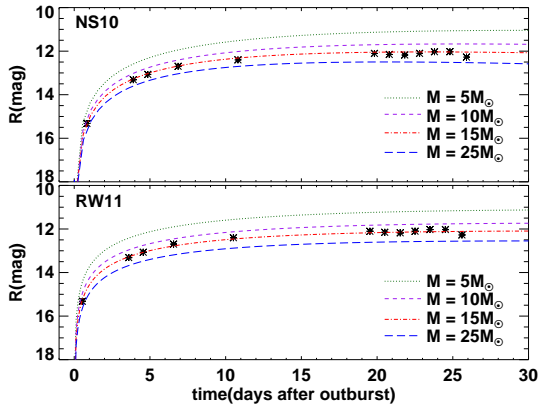


Fig. 6. Zoom in of the optical lightcurves of SN 1998S in comparison to the analytical model of NS10(top panel with $R = 300R_{\odot}$ and $E = 8.75 \times 10^{51}$ ergs) and RW11(bottom panel with $R = 2000R_{\odot}$ and $E = 3.0 \times 10^{51}$ ergs) with different masses. The dates of explosion for NS10 and RW11 in the figure are JD 2450874.34 and JD 2450874.64 respectively.

NS10, but different lightcurves show similar trends and can fit the data by adding a constant.

From the previous results, radius seems to have a more important impact in the shape of lightcurves. In figure 8, we try to fit our data using both models, each with the best fitting radius, different masses and the best corresponding energy. In both models, a bigger mass requires a bigger energy. With suitable combination of mass and energy, similar lightcurves can be produced. For the mass of 5 to 25 M_{\odot} , the corresponding energy range which can fit the data is 3.5×10^{51} to 13.5×10^{51} ergs for NS10 and 1.25×10^{51} to 4.5×10^{51} ergs for RW11. These ranges are reasonable for a red supergiant. Both NS10 and RW11 can constrain the radius but cannot distinguish between different combinations of mass and energy. We note that for RW11, the lightcurves for $R = 2000R_{\odot}$, $M = 5M_{\odot}$ and $E = 1.25 \times 10^{51}$ ergs can fit our data well enough. This modelling result is consistent with Chugai(2001) in which he assumed $R = 2.4 \times 10^{14}$ cm ($\sim 3500R_{\odot}$), $M = 5M_{\odot}$ and $E = 1.1 \times 10^{51}$ ergs.

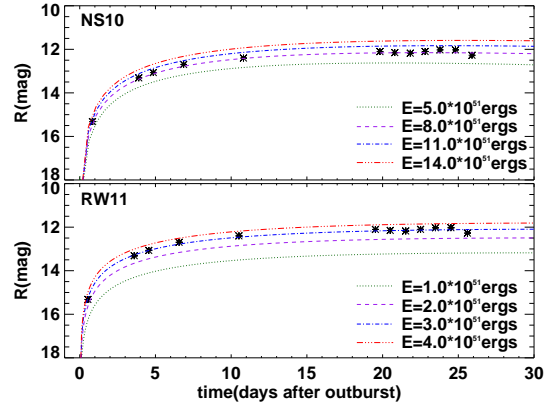


Fig. 7. Zoom in of the optical lightcurves of SN 1998S in comparison to the analytical model of NS10(top panel with $R = 300R_{\odot}$ and $M = 15M_{\odot}$ ergs) and RW11(bottom panel with $R = 2000R_{\odot}$ and $M = 15M_{\odot}$) with different energies. The dates of explosion for NS10 and RW11 in the figure are JD 2450874.34 and JD 2450874.64 respectively.

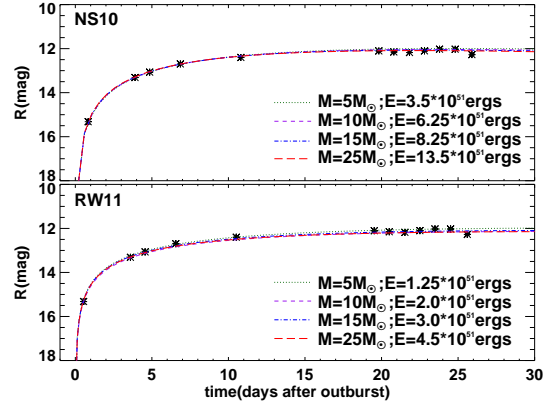


Fig. 8. Zoom in of the optical lightcurves of SN 1998S in comparison to the analytical model of NS10(top panel with $R = 300R_{\odot}$) and RW11(bottom panel with $R = 2000R_{\odot}$). For each model, the lightcurves for different masses and the best corresponding energy are shown. The dates of explosion for NS10 and RW11 in the figure are JD 2450874.34 and JD 2450874.64 respectively.

We try to compare the temperatures derived from both models to that of SN 1998S, which are estimated by blackbody fit. In figure 1, we plot the temperatures for both models using the best fitting parameters derived in figure 4. Both models predict a lower temperature than the data. We also try to fit the temperatures using different sets of parameters. The best fit for NS10 predicts a temperature of ~ 67000 K on the day of discovery, which amounts to ~ 0.011 in the term $i_3(V_{SN} - I_{SN})$ of equation(2). For RW11, the temperature found for this day is ~ 55000 K. This also amounts to ~ 0.011 for the above-mentioned term. Since this value differs from the error we quote by a magnitude of 0.001, even if the temperature is really that high, the results are still not affected.

4. Discussion and Conclusion

We present early photometry of SN 1998S in this work and use analytical models to fit our data. The dates of explosion derived from both models agree with each other very well, only with a

small difference of 0.3 day. For NS10, the date of explosion is 1998 March 1.84(JD 2450874.34) and it is 1998 March 2.14(JD 2450874.64) for RW11. In NS10, the lightcurves show a bump in the very early phase which is the transition between the planar and the spherical phase. This bump indicates the magnitude during transition, which is an important constraint to the parameters. At the very early phase after supernova explosion, the energy concentrates on the high energy band. If our first data point was taken in the U band instead of unfiltered, we may be able to better constrain the parameters of the supernova. GALEX detected UV emission(<1 day) from SNe SNLS-04D2dc and SNLS-06D1jd(Gezari et al. 2008). The authors model the very early lightcurves up to 55 hours and find the mass loss to be $\sim 10^{-3}M_{\odot} \text{ yr}^{-1}$. We took four data points during the first 10 days, with the first one taken within one day after explosion. This sampling frequency is dense enough and is significant in determining the parameters.

Both NS10 and RW11 for an RSG can fit the early lightcurves well. In NS10, the breakout is observed and then followed by a broken power-law decay of the luminosity in the planar phase. Then in the spherical phase, the luminosity rises again until the frequency range peaks in the blackbody spectrum. The transition between the planar and spherical phases causes the early bump in the analytical lightcurves. This bump is not observed in RW11 since this model has got only one phase. In the upper panel of fig.4(NS10), a larger radius results in a longer planar phase and a brighter magnitude at the transition. The duration of the planar phase and the magnitude at transition are important in constraining the model parameters. However, this very early phase is not considered in RW11 and the result may be different if the breakout phase is considered in this model. From the results of the fit, we find the radius of the progenitor to be $\sim 300R_{\odot}$ (NS10) and $\sim 2000R_{\odot}$ (RW11). The later result is consistent with Chugai(2001). The ranges of mass and energy found from both models are within that of a red supergiant. These two models derive quite different parameters.

The temperatures derived from both models cannot fit the data well. We can only obtain a satisfactory fit with different sets of parameters for both models. The derived temperatures would be a lot higher than our extrapolated result. However, this would only contribute to a small change of a magnitude of ~ 0.001 in the error. The final result is not really affected.

Acknowledgements. The authors thank E. Nakar and J. S. Deng for helpful discussions.

References

- Arnett, W. D., 1980, ApJ, 237, 541
 Arnett, W. D., 1982, ApJ, 253, 785
 Arnett, W. D., Fu, A., 1989, ApJ, 340, 396
 Barbon R., Ciatti F., Rosino L., 1979, A&A 72, 287
 Bowen, D., Roth, K. C., Meyer, D. M. et al., 2000, ApJ, 536, 225
 Chugai, N. N. 1992, SvA, 36, 63.
 Chugai, N. N. 2001, MNRAS, 326, 1448
 Fassia A., et al., 2000, MNRAS, 318, 1093
 Filippenko A.V., Moran E.C., 1998, IAU Circ. 6829
 Fransson, C., & Chevalier, R. A. 1987, ApJ, 322, L15
 Gezari, S., Rest, A., Huber, M. E. et al. 2010, ApJ, 720, 77
 Leonard D. C., Filippenko A. V., Barth A. J., Matheson T., 2000, ApJ, 536, 239
 Li, W.-d., & Li, C. 1998, IAUC, 6829
 Liu Q.-Z., Hu J.-Y., Hang H.-R., Qiu Y.-L., Zhu Z.-X., Qiao Q.-Y., 2000, A&ASS, 144, 219
 Modjaz, M., Li, W., Butler, N. et al., 2009, ApJ, 702, 226
 Nakar, E., & Sari, R. 2010, ApJ, 725, 904
 Pooley, D., Lewin, W. H. G., Fox, D. W., et al. 2002, ApJ, 572, 932
 Rabinak, I., & Waxman, E. 2011, ApJ, 728, 63
 Schlegel E. M., 1990, MNRAS, 244, 269

- Soderberg, A. M., Berger, E., Page, K. L., et al. 2008, Nature, 453, 469
 Waxman, E., Meszaros, P., & Campana, S. 2007, ApJ, 667, 351

Table 1. Standard Magnitudes and Temperatures of SN 1998S($t_{exp} = \text{JD } 2450874.49$)

Day	Julian Day(2450000+)	B band	V Band	R Band	Temperature(K)
0.69	875.18	-	-	15.32 (0.11)	-
3.75	878.24	13.06 (0.06)	13.29 (0.01)	13.31 (0.02)	23000 (7500)
4.71	879.20	12.72 (0.06)	13.08 (0.01)	13.07 (0.02)	22000 (6500)
6.71	881.20	12.60 (0.05)	12.74 (0.01)	12.70 (0.01)	21000 (6000)
10.66	885.15	12.32 (0.05)	12.39 (0.01)	12.40 (0.01)	16000 (4100)
19.68	894.17	12.38 (0.04)	12.31 (0.01)	12.11 (0.01)	13000 (2800)
20.66	895.15	12.51 (0.03)	12.28 (0.01)	12.15 (0.01)	12000 (2400)
21.68	896.17	12.45 (0.04)	12.34 (0.01)	12.18 (0.01)	11000 (2200)
22.66	897.15	12.64 (0.04)	12.45 (0.02)	12.10 (0.01)	11000 (6000)
23.64	898.13	13.00 (0.04)	12.48 (0.01)	12.03 (0.02)	10000 (2000)
24.66	899.15	12.92 (0.04)	12.44 (0.02)	12.03 (0.02)	10000 (1800)
25.75	900.24	12.84 (0.14)	12.68 (0.05)	12.27 (0.45)	9700 (2600)

Table 2. Residuals of the models of NS10 and RW11 using different parameters

Julian Day(2450000+)	NS10				RW10			
	modal 1	modal 2	modal 3	modal 4	modal 1	modal 2	modal 3	modal 4
875.18	-0.05	0.02	0.15	0.22	-0.15	-0.07	0.00	0.00
878.24	-0.02	-0.01	0.03	0.01	-0.04	-0.04	-0.03	-0.06
879.20	-0.01	-0.01	0.01	-0.04	0.01	0.00	-0.00	-0.05
881.20	0.05	0.01	-0.01	-0.10	0.12	0.08	0.04	-0.00
885.15	0.02	-0.09	-0.15	-0.32	0.14	0.06	-0.02	-0.09
894.17	0.15	-0.03	-0.26	-0.58	0.24	0.07	-0.09	-0.19
895.15	0.10	-0.08	-0.33	-0.66	0.18	0.01	-0.16	-0.26
896.17	0.08	-0.11	-0.37	-0.72	0.16	-0.03	-0.20	-0.31
897.15	0.16	-0.04	-0.32	-0.68	0.23	0.03	-0.14	-0.26
898.13	0.25	0.04	-0.25	-0.63	0.31	0.10	-0.08	-0.20
899.15	0.26	0.04	-0.26	-0.66	0.31	0.09	-0.10	-0.22
900.24	0.03	-0.20	-0.52	-0.93	0.06	-0.16	-0.36	-0.49

NS10:

 Modal 1: $R = 200R_{\odot}$; $M = 5M_{\odot}$; $E = 4.0 \times 10^{51}$ ergs

 Modal 2: $R = 300R_{\odot}$; $M = 15M_{\odot}$; $E = 8.75 \times 10^{51}$ ergs

 Modal 3: $R = 500R_{\odot}$; $M = 15M_{\odot}$; $E = 7.5 \times 10^{51}$ ergs

 Modal 4: $R = 1000R_{\odot}$; $M = 20M_{\odot}$; $E = 9.0 \times 10^{51}$ ergs

RW10:

 Modal 1: $R = 1000R_{\odot}$; $M = 5M_{\odot}$; $E = 1.5 \times 10^{51}$ ergs

 Modal 2: $R = 2000R_{\odot}$; $M = 15M_{\odot}$; $E = 3.0 \times 10^{51}$ ergs

 Modal 3: $R = 3500R_{\odot}$; $M = 15M_{\odot}$; $E = 2.5 \times 10^{51}$ ergs

 Modal 4: $R = 5000R_{\odot}$; $M = 25M_{\odot}$; $E = 3.0 \times 10^{51}$ ergs